Electronic Supplementary Material (ESI) for CrystEngComm.
This journal is © The Royal Society of Chemistry 2022

Electronic supplementary information

A family of oxime-based titanium-oxo clusters: synthesis, structures, and photoelectric responses

Chao Wang*, Ning Chen, Fangong Kong and Shoujuan Wang

State Key Laboratory of Biobased Material and Green Papermaking, Qilu University of Technology (Shandong Academy of Sciences), Jinan, 250353, China, E-mail: wangchao@qlu.edu.cn

1. Experimental section

Materials and Characterization. All the starting reagents employed were bought commercially and were used directly without further purification. Titanium isopropoxide (97%), salicylaldoxime (98%), and salicylhydroxamic acid (99%) were bought from Aladdin. The solid-state optical diffuse reflectance data were collected using a Cary 4000 UV–vis spectrophotometer. The infrared spectra (IR) data was recorded on a Nicolet 6700 spectrometer. The powder X–ray diffractometer (pXRD) data was collected on a Bruker D_8 Focus pXRD diffractometer (Cu–Kα, λ=1.5405 nm) was used to collect the pXRD data. The thermogravimetric analysis (TGA) data was recorded on a TGAQ50 thermal analysis instrument. Elemental analysis (C, H and N) was performed using a Vario EL III elemental analyzer.

Photocurrent Measurement. The electrochemical workstation (CHI650) in a standard three−electrode electrochemical cell with a working electrode, a reference electrode (Ag/AgCl electrode), and a counter electrode (Pt electrode) was used for photocurrent measurements. All of the tests were carried out in the Na_2SO_4 (0.2 M) aqueous solution. The working electrode in this paper was obtained by solution spin coating. The colloidal dispersion was obtained by ultrasonic treatment of fresh crystal sample (5 mg) in ethanol (1 mL), and then coating the dispersion on the cleaned FTO glass (0.1 cm^2 area). The working electrode was obtained after evaporation. A high−pressure xenon lamp (300 W) was used as light source.

2. Crystallographic details

Single-crystal structure determinations. Crystallographic data were collected an Agilent Gemini E dual-light source X-ray single crystal diffractometer with Eos CCD detector. The CCDC numbers of **1**−**5** are 2091421−2091425, and the specific crystallographic information can be received from the Cambridge Crystallographic Data Centre. The structures are solved by the inherent phase method in the SHELXT[1] program, and refined by the least square method in the SHELXL[1] program. Both programs are used coupling with OLEX2[2]. All non-hydrogen atoms, including free solvent and host molecules, are directly identified by the SHELXT program and refined by anisotropically. The RIGU, ISOR, and DFIX restrains were necessary to

make the structural models more reasonable. Crystallographic data for clusters **1**−**6** are summarized in Table S1.

Table S1. X-ray measurements and structure solution of clusters **1**−**5**.

Cluster	**1**	**2**	**3**
Empirical formula	$C_{44}H_{34}C_{l4}N_6O_{12}Ti_3$	$C_{27}H_{29}N_3O_8Ti_2$	$C_{32}H_{32}N_2O_{13}Ti_3$
Formula weight	1124.27	619.33	796.29
Crystal system	Triclinic	monoclinic	monoclinic
Space group	P-1	$P2_1/n$	$P2_1/c$
a/Å	9.2333(5)	13.6916(7)	12.5281(11)
b/Å	10.1635(8)	14.6046(9)	30.0488(17)
c/Å	14.3186(5)	14.2100(8)	10.1629(9)
α/°	79.464(5)	90	90
β/°	74.926(4)	101.132(5)	110.549(11)
γ/°	64.319(6)	90	90
V	1165.49(13)	2788.0(3)	3582.4(5)
Z	1	4	2
ρ_{calc}/g·cm^{-3}	1.602	1.476	1.476
μ(MoKα)/mm^{-1}	6.978	5.337	6.129
F(000)	570.0	1280.0	1632.0
Reflections collected/unique	7342/4349	10646/5288	13917/6819
Data/restraints/parameters	4349/25/313	5288/0/365	6819/0/455
R_1/wR_2(I>2σ(I))[a]	0.0679/0.2090	0.0627/0.1601	0.0692/0.1564
R_1/wR_2(all data)	0.0757/0.2304	0.0900/0.1901	0.1382/0.2034
GooF(all data)[b]	1.064	1.060	0.988

Cluster	**4**	**5**
Empirical formula	$C_{41}H_{39}N_3O_{13}Ti_3$	$C_{64}H_{100}N_4O_{28}Ti_8$
Formula weight	925.45	1756.67
Crystal system	monoclinic	Triclinic
Space group	P21/n	P-1
a/Å	11.8670(3)	13.5956(5)
b/Å	21.1077(5)	14.9312(5)
c/Å	18.0596(4)	20.3151(7)
α/°	90	93.9774(15)
β/°	106.6678(9)	95.1157(14)
γ/°	90	100.3300(15)
V	4333.59(18)	4025.6(2)
Z	4	2
ρ_{calc}/g·cm^{-3}	1.418	1.449
μ(MoKα)/mm^{-1}	0.605	0.828
F(000)	1904.0	1824.0
Reflections collected/unique	61884/8876	75194/16460
Data/restraints/parameters	8876/63/565	16460/102/991
R_1/wR_2(I>2σ(I))[a]	0.0342/0.0883	0.0477/0.1256
R_1/wR_2(all data)	0.0472/0.0971	0.0684/0.1416
GooF(all data)[b]	1.037	1.019

[a] $R_1 = \sum||Fo|-|Fc||/\sum|Fo|$; $wR_2 = \{\sum w[(Fo)^2-(Fc)^2]^2/\sum w[(Fo)^2]^2\}^{1/2}$

[b] $GooF = \{\sum w[(Fo)^2-(Fc)^2]^2/(n-p)\}^{1/2}$

3. Powder X-ray diffraction

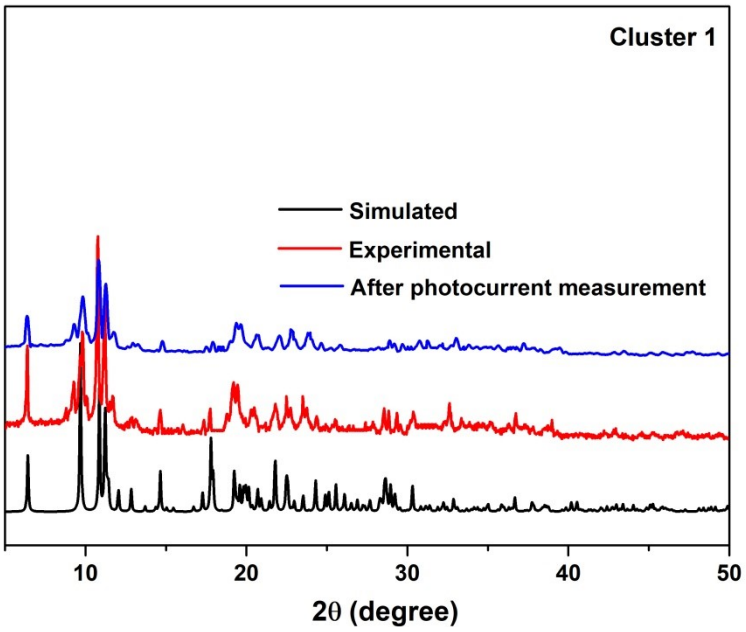

Figure S1. The XRD patterns of cluster **1**.

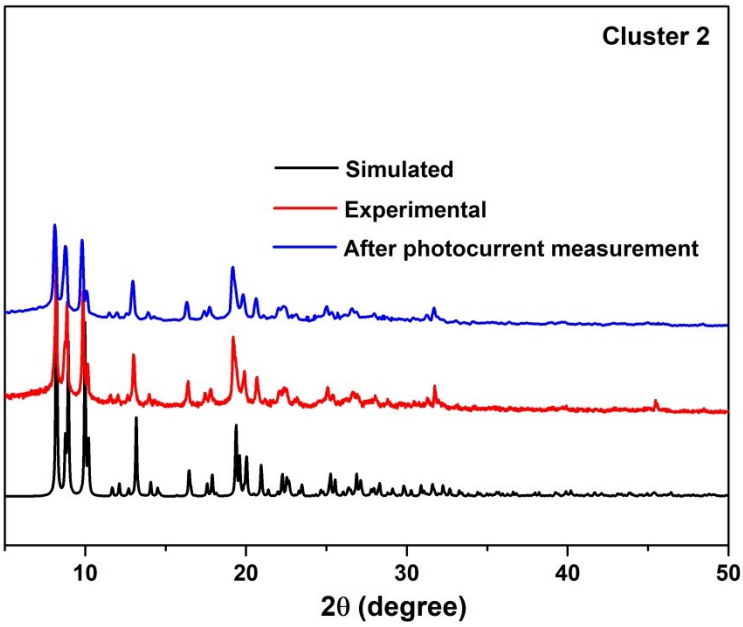

Figure S2. The XRD patterns of cluster **2**.

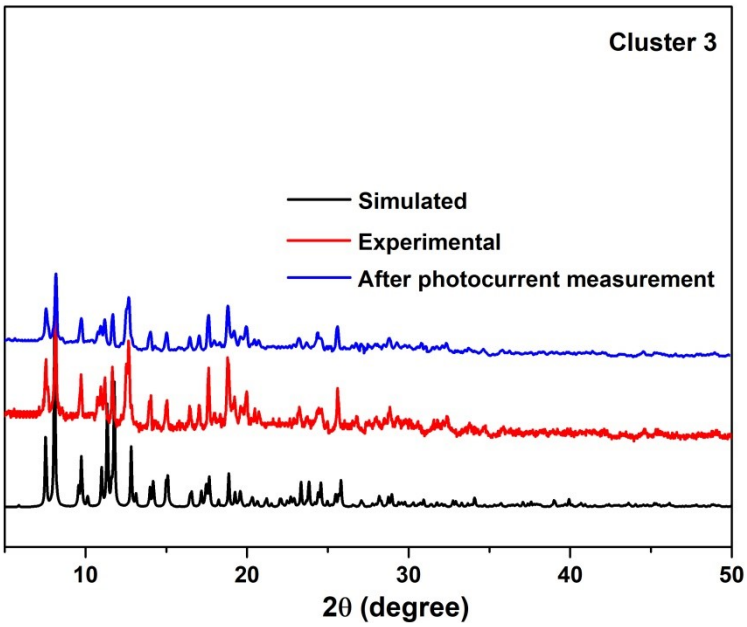

Figure S3. The XRD patterns of cluster **3**.

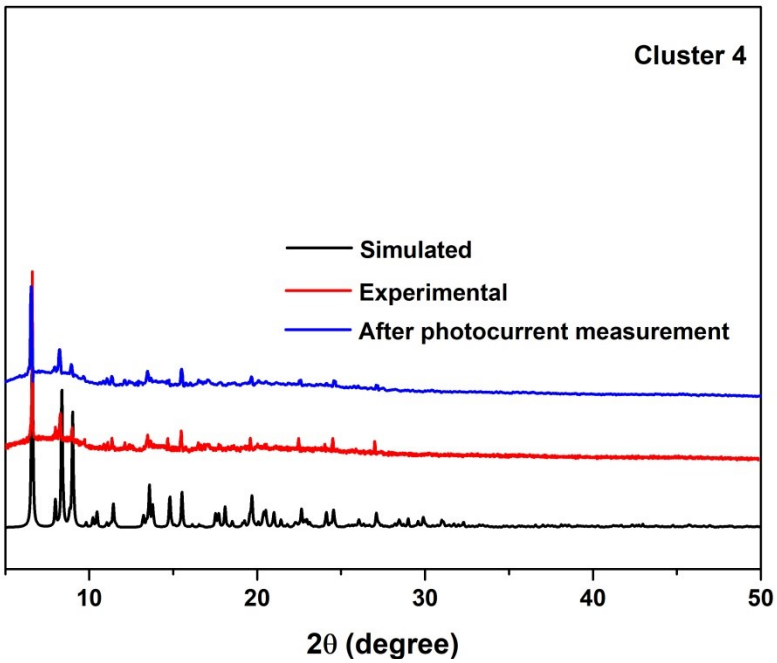

Figure S4. The XRD patterns of cluster **4**.

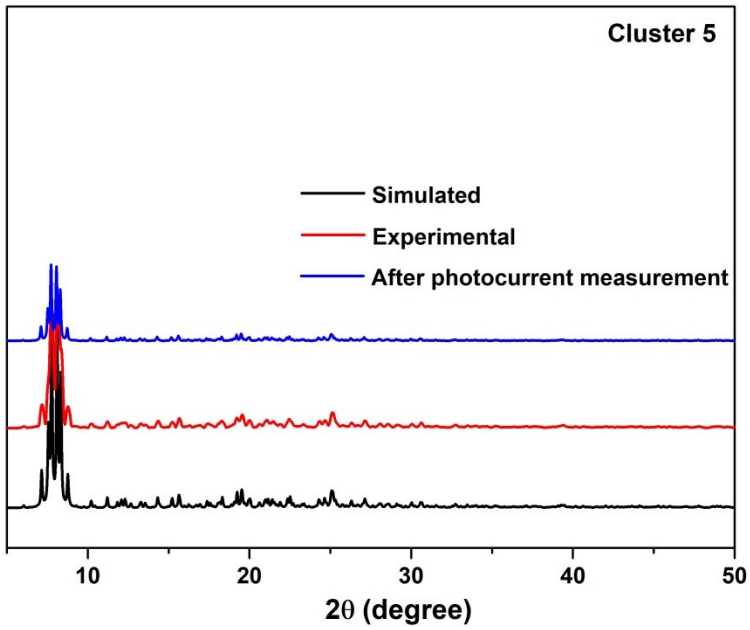

Figure S5. The XRD patterns of cluster **5**.

4. Thermogravimetric measurement

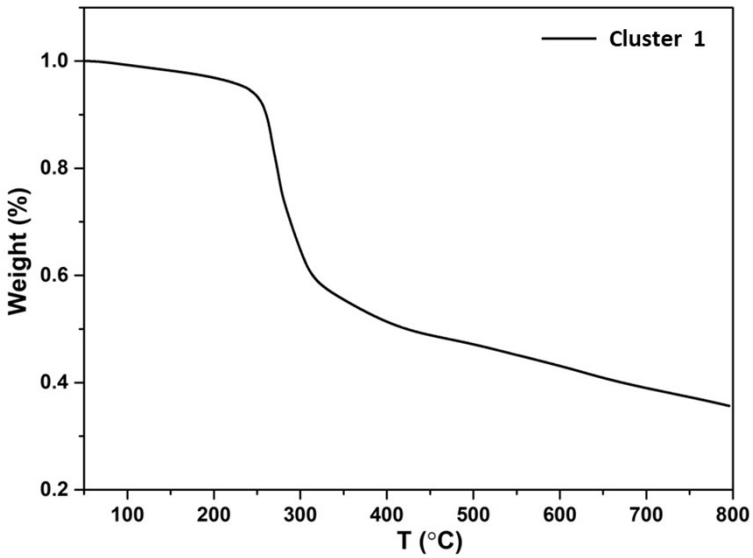

Figure S6. Thermal decomposition curve of cluster **1**.

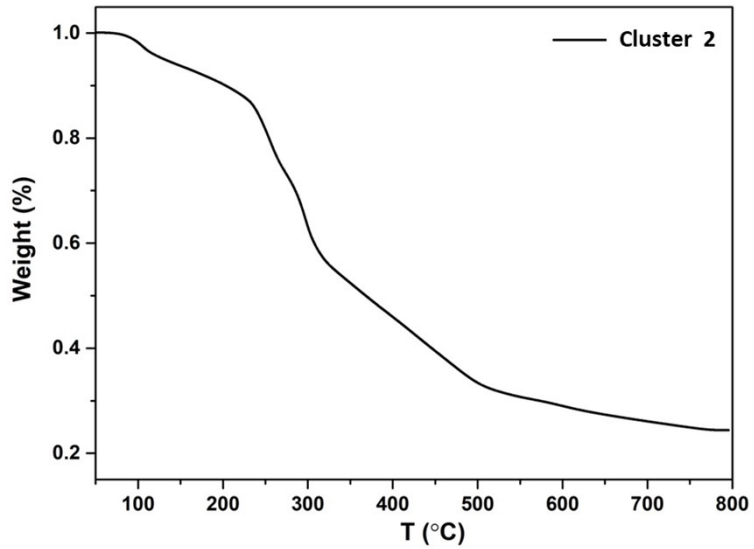

Figure S7. Thermal decomposition curve of cluster **2**.

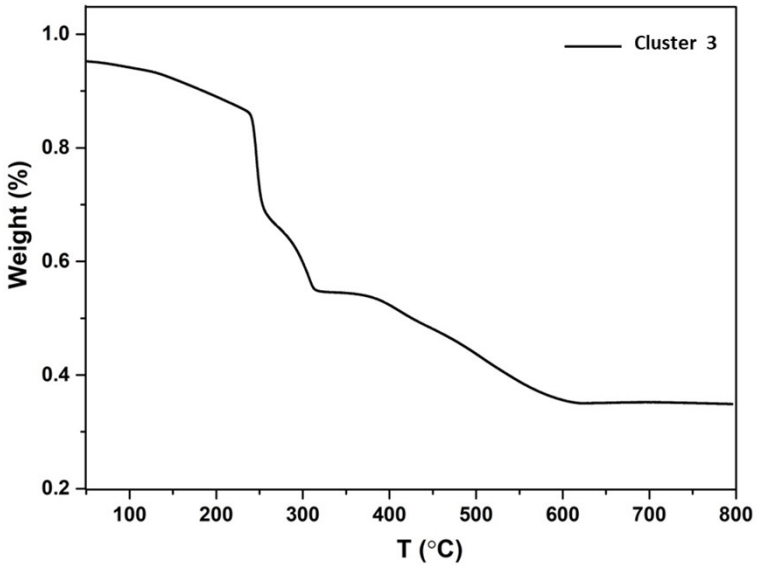

Figure S8. Thermal decomposition curve of cluster **3**.

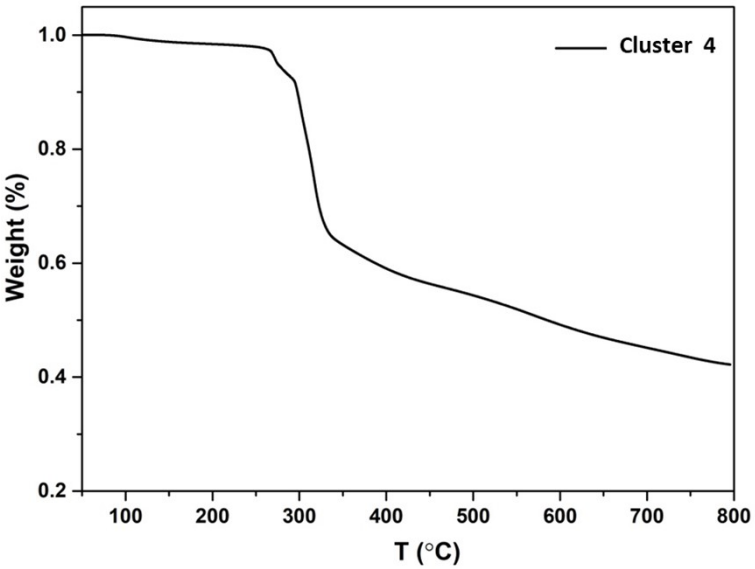

Figure S9. Thermal decomposition curve of cluster **4**.

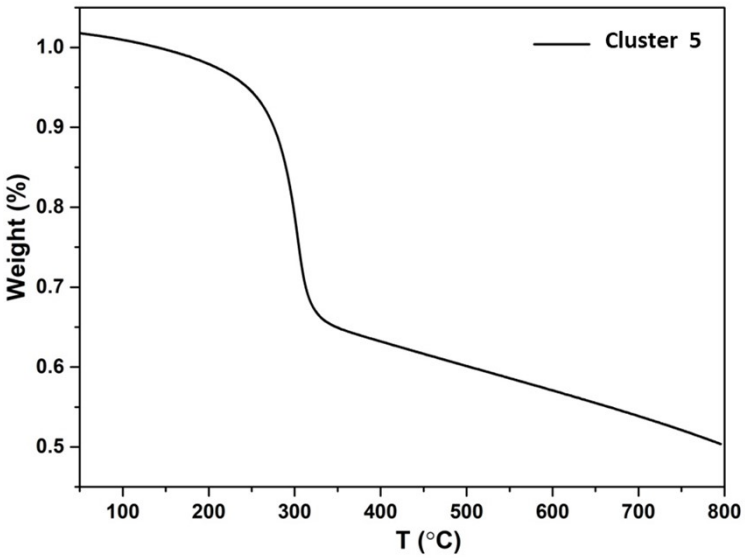

Figure S10. Thermal decomposition curve of cluster **5**.

5. Fourier transform infrared spectra

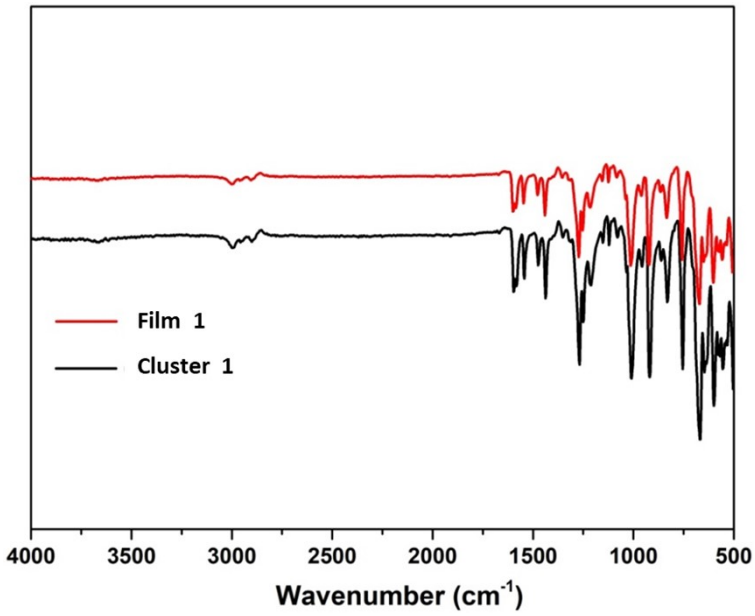

Figure S11. The FTIR spectra of cluster **1** and the sample after photoelectrochemical experiment.

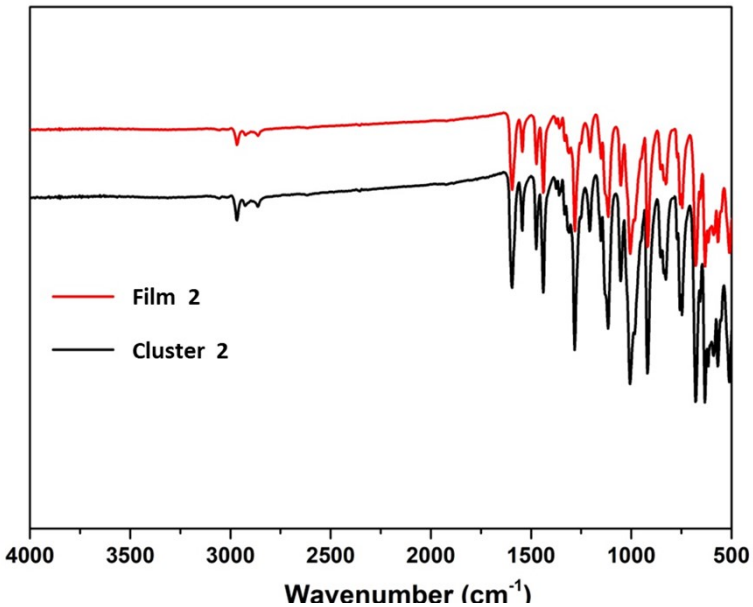

Figure S12. The FTIR spectra of cluster **2** and the sample after photoelectrochemical experiment.

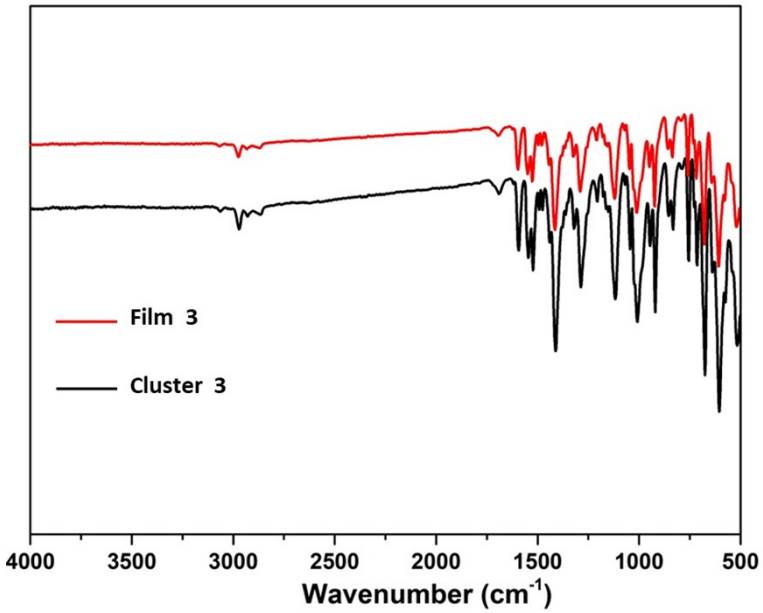

Figure S13. The FTIR spectra of cluster **3** and the sample after photoelectrochemical experiment.

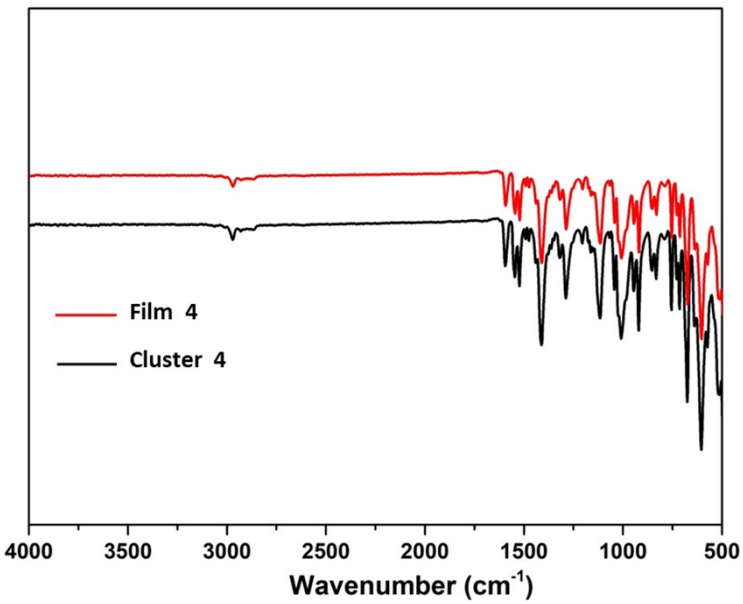

Figure S14. The FTIR spectra of cluster **4** and the sample after photoelectrochemical experiment.

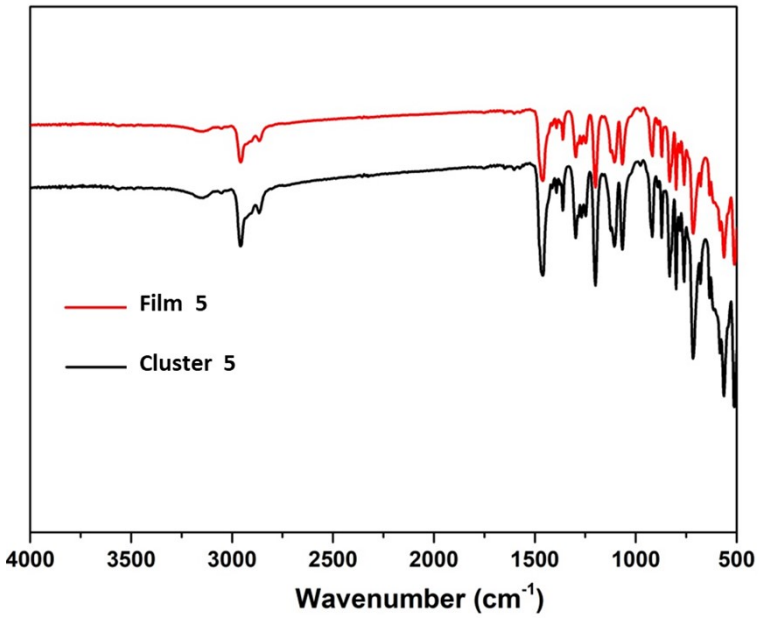

Figure S15. The FTIR spectra of cluster **5** and the sample after photoelectrochemical experiment.

6. The optical band gap

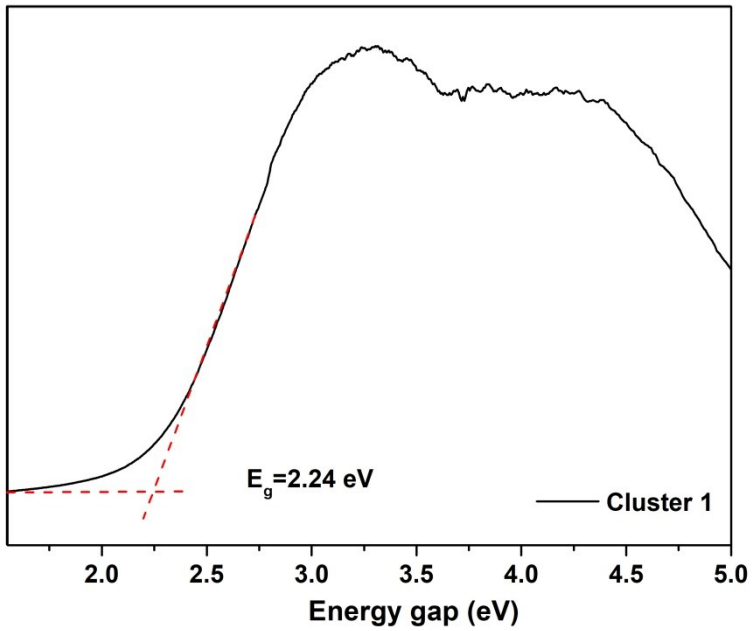

Figure S16. The optical band gap of cluster **1**.

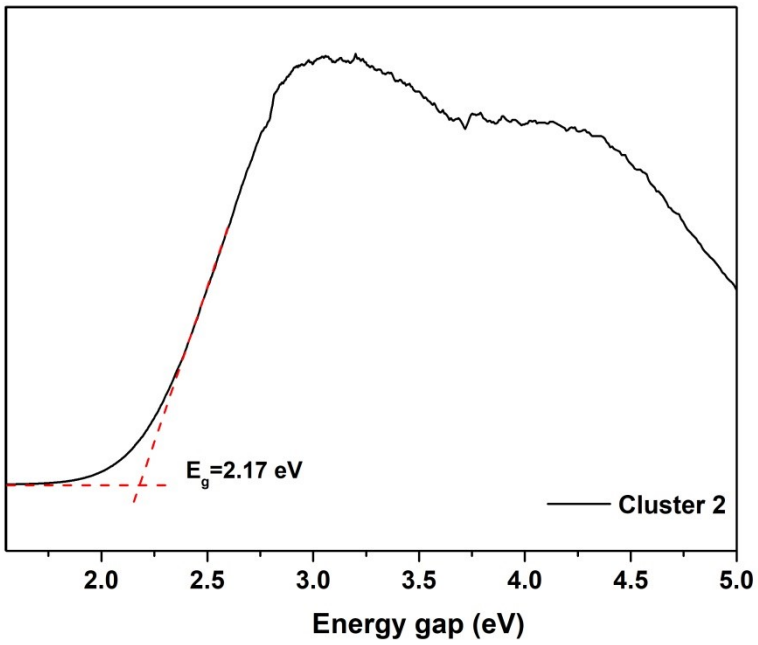

Figure S17. The optical band gap of cluster **2**.

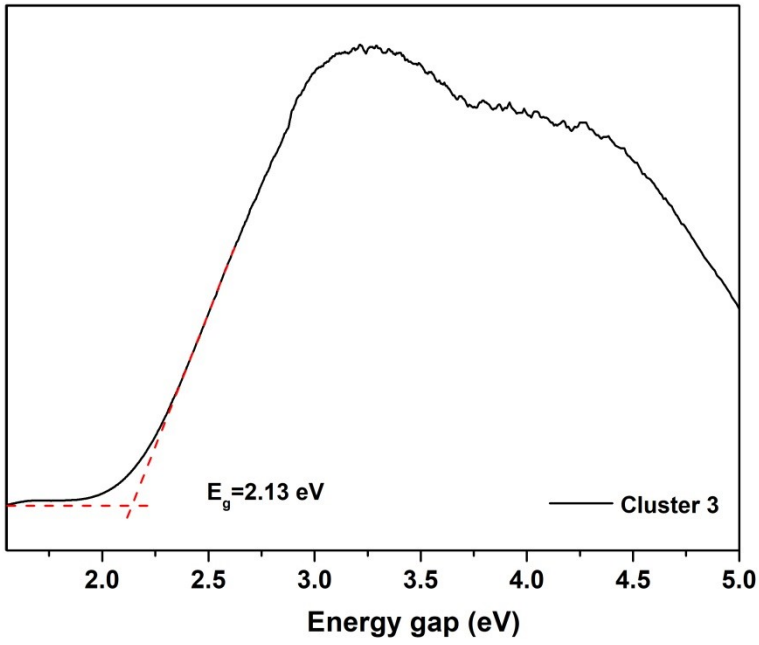

Figure S18. The optical band gap of cluster **3**.

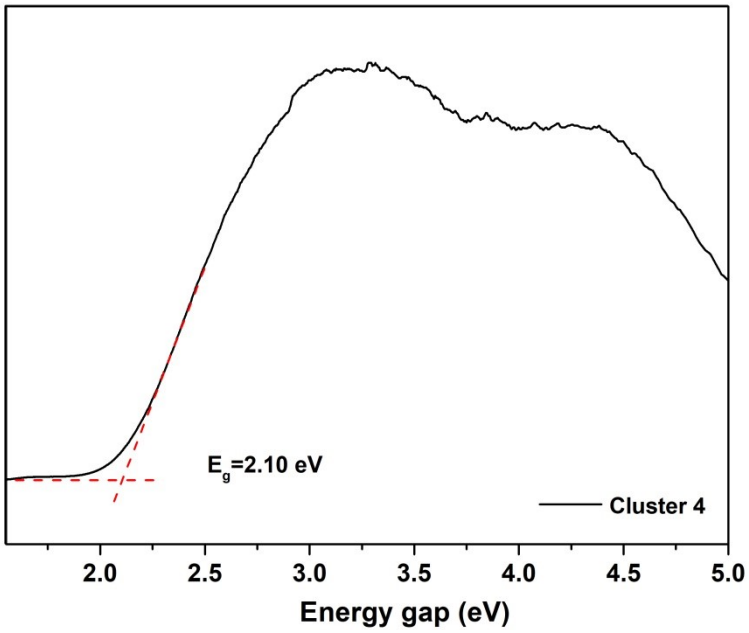

Figure S19. The optical band gap of cluster **4**.

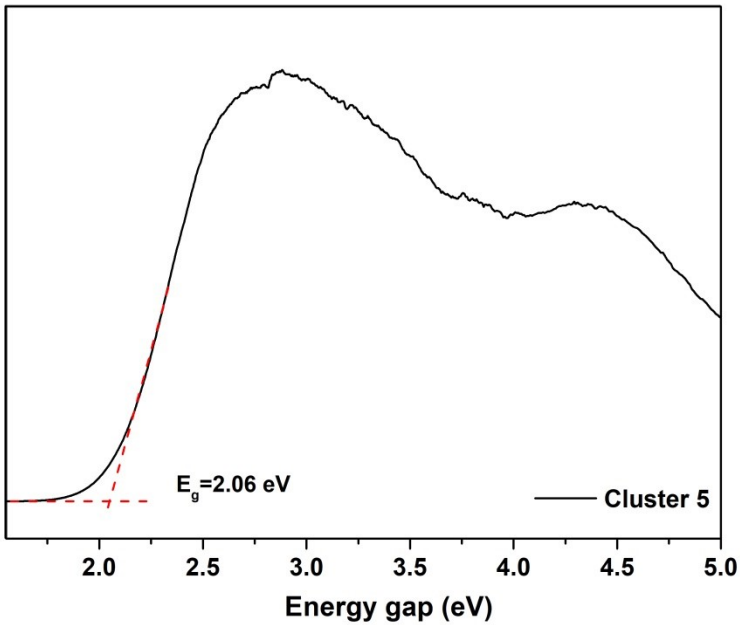

Figure S20. The optical band gap of cluster **5**.

7. **Photocurrent responses**

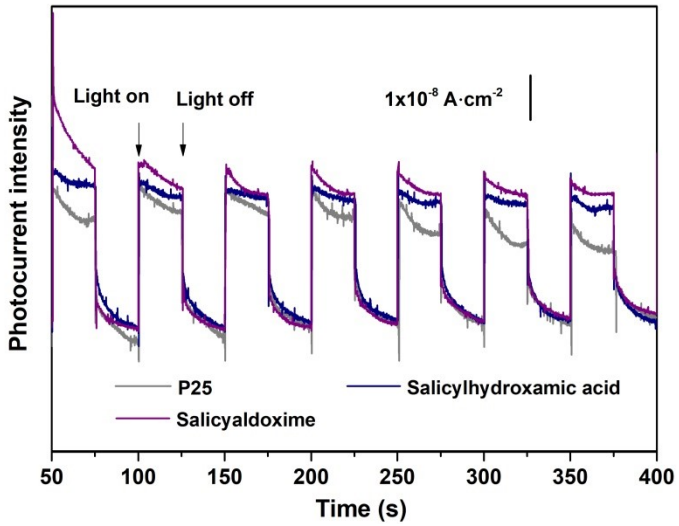

Figure S21. Photocurrent responses of electrodes derived from TiO_2 and ligands.

8. **Mott-Schottky plots**

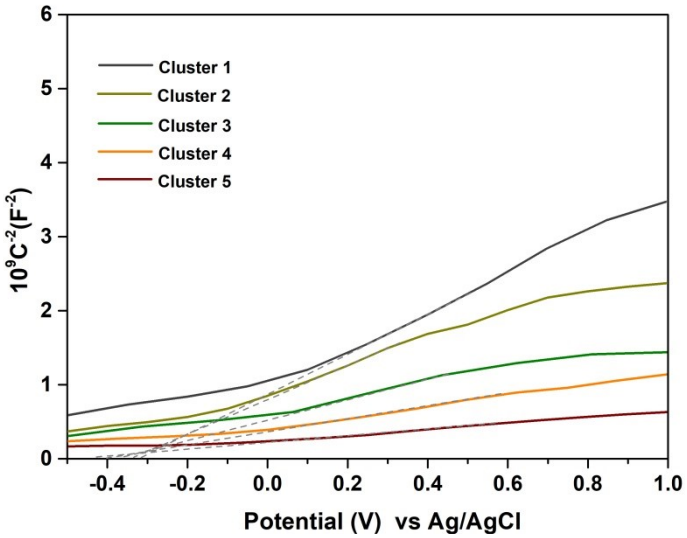

Figure S22. Mott–Schottky plots of the photoelectrodes at frequency of 1000 Hz.

References

1. Sheldrick, G. M. Crystal Structure Refinement with SHELXL. *Acta Cryst.* **2015**, C71, 3-8.
2. Dolomanov, O. V.; Bourhis, L. J.; Gildea, R. J.; Howard, J. A. K.; Puschmann, H. OLEX2: A Complete Structure Solution, Refinement and Analysis Program. *J. Appl. Crystallogr.* **2009**, 42, 339-341.